COMPRESSED CYCLOSTATIONARY DETECTION FOR COGNITIVE RADIO

Deborah Cohen and Yonina C. Eldar

Technion - Israel Institute of Technology, EE department
Haifa, Israel
{debby@campus, yonina@ee}.technion.ac.il

ABSTRACT

Cognitive Radio requires both efficient and reliable spectrum sensing of wideband signals. In order to cope with the sampling rate bottleneck when dealing with such signals, sub-Nyquist methods have been proposed. However, these techniques decrease the signal to noise ratio (SNR) due to aliasing effects. Cyclostationary detection, which exploits the periodic property of communication signal statistics, absent in stationary noise, is a natural candidate for this setting. In this work, we consider cyclic spectrum recovery from sub-Nyquist samples, in order to achieve both efficiency and robustness to noise. We show how the cyclic spectrum can be recovered directly from the low rate samples, even for non sparse signals, and derive a lower bound on the sampling rate required for perfect cyclic spectrum recovery in the presence of stationary noise. Simulations show that cyclostationary detection outperforms energy detection in low SNRs in the sub-Nyquist regime.

Index Terms— Cyclostationarity, sub-Nyquist sampling, cognitive radio, compressed sensing

I. INTRODUCTION

Spectrum sensing has recently been facing new challenges due, to a large extent, to cognitive radio (CR) applications [1]. Today, CRs are perceived as a potential solution to the spectrum over-crowdedness [2]. Even though most of the spectrum is already owned and new users can hardly find free frequency bands, various studies [3]–[5] have shown that it is typically significantly underutilized. CRs would allow secondary users to opportunistically use the licensed spectrum when the corresponding primary user (PU) is not active [1]. To comply with CR's requirements, spectrum sensing has to be efficient and performed in real time while being reliable and able to cope with low signal to noise ratio (SNR) regimes.

In order to efficiently sample sparse wideband signals, such as those CRs have to deal with, several sampling methods have recently been proposed [6]–[9] that recover a multiband signal or its power spectrum [10]–[12] from sub-Nyquist samples. All these approaches rely on energy detection. Unfortunately, the sensitivity of energy detection is amplified when performed on sub-Nyquist samples due to aliasing of the noise [13]. Therefore, this scheme fails to meet CR performance requirements in low SNR regimes. Cyclostationary detection, which exploits a statistical property of communication signals, is thus a natural candidate for spectrum sensing from sub-Nyquist samples in low SNRs.

Cyclostationary processes have statistical characteristics that vary periodically, arising from the underlying data modulation mechanisms, such as carrier modulation, periodic keying or pulse modulation. The cyclic spectrum, a characteristic function of such processes, exhibits spectral peaks at certain frequency locations called cyclic frequencies, which are determined by the signal parameters, particularly the carrier frequency and symbol rate [14]. Stationary noise and interference exhibit no spectral correlation [14], which makes cyclostationary detectors robust to noise.

Signal detection using cyclostationarity and its application to spectrum sensing for CR in the Nyquist regime, has been thoroughly investigated; see e.g., [2], [15]–[17]. Recently, cyclostationary detection from sub-Nyquist samples was treated in [18]–[21]. A general framework is adopted, that exploits a linear relation between the sub-Nyquist and Nyquist samples, over a finite sensing time. In particular, a transformation between the Nyquist cyclic spectrum and the time-varying correlations of the sub-Nyquist samples is derived to retrieve the former from the latter. The main drawback of this digital approach is that it does not deal with the analog sampling scheme itself, in which we do not have access to the Nyquist samples. In addition, finite sensing time requires the assumption that the cyclic frequencies lie on a predefined grid. The theoretical resolution that can be achieved is thus dictated by the sensing time, which is an inherent parameter of the sampling and reconstruction scheme, and not only a practical design parameter. Moreover, no theoretical guarantees on the minimal sampling rate allowing for perfect recovery of the cyclic spectrum have been given.

In [22], a concrete sampling scheme is considered, known as multicoset, or non-uniform sampling. The authors derive conditions on the system matrix to have full rank, allowing for perfect cyclic spectrum reconstruction from the compressive measurements. While real sampling schemes are considered here, the theoretical cyclic spectrum resolution still depends on the sensing time. The gridding, or discretization, is part of the theoretical derivations.

In this work, we propose to reconstruct the signal's cyclic spectrum from sub-Nyquist samples obtained using the modulated wideband converter (MWC) [7]. Our theoretical approach does not involve discretization or gridding and the cyclic spectrum can be recovered at any frequency. In addition, the MWC analog front-end is a practical sampling scheme that has been implemented in hardware [23]. We perform cyclostationarity detection on the sub-Nyquist samples, thereby obtaining both an efficient, fast and frugal detector and one that is reliable and robust to noise. We derive a sampling rate bound allowing for perfect recovery of the cyclic spectrum in our settings, both for sparse and non sparse signals. We note that the cyclic spectrum can be perfectly recovered in the presence of stationary noise, from compressed samples, except for a limited number of cyclic frequencies that are multiples of the basic low sampling rate. For those, the reconstruction is performed in the presence of bounded noise. Simulations show that cyclostationary detection outperforms energy detection in sub-Nyquist regimes, in low SNR.

This paper is organized as follows. In Section II, we describe the cyclostationary multiband model. Sections III and IV present the sub-Nyquist sampling and cyclic spectrum reconstruction algorithms and conditions, respectively. Numerical experiments are reported in Section V.

This project has received funding from the European Union's Horizon 2020 research and innovation program under grant agreement No. 646804-ERC-COG-BNYQ, and from the Israel Science Foundation under Grant no. 335/14. Deborah Cohen is grateful to the Azrieli Foundation for an Azrieli Fellowship.

II. CYCLOSTATIONARY MULTIBAND MODEL

II-A. Multiband Model

Let $x(t)$ be a real-valued continuous-time signal, supported on $\mathcal{F} = [-1/2T_{\text{Nyq}}, +1/2T_{\text{Nyq}}]$ and composed of up to N_{sig} uncorrelated cyclostationary transmissions corrupted by additive noise, such that

$$x(t) = \sum_{i=1}^{N_{\text{sig}}} s_i(t) + n(t). \tag{1}$$

Here $n(t)$ is a wide-sense stationary bandpass noise and $s_i(t)$ is a zero-mean cyclostationary bandpass process, as defined below, with carrier frequency f_i and bandwidth B_i. The number of transmissions N_{sig}, their carrier frequencies f_i, bandwidths B_i and modulations are unknown. The single-sided bandwidth of each transmission is only assumed to not exceed a known maximal bandwidth B, namely $B_i \leq B$ for all $1 \leq i \leq N_{\text{sig}}$.

Denote by $f_{\text{Nyq}} = 1/T_{\text{Nyq}}$ the Nyquist rate of $x(t)$. If the bandwidth is fully occupied, then it holds that $N_{\text{sig}}B$ is of the order of f_{Nyq}. In multiband settings, where $N_{\text{sig}}B \ll f_{\text{Nyq}}$ and $x(t)$ is thus sparse in frequency, we show that the sampling rate for perfect cyclic spectrum reconstruction can be further reduced. For convenience, we denote by $K = 2N_{\text{sig}}$ the upper bound on the number of occupied bands, to account for both the positive and negative frequency bands.

II-B. Cyclostationarity

A process $s(t)$ is said to be cyclostationary with period T_0 in the wide sense if its mean $\mathbb{E}[s(t)] = \mu_s(t)$ and autocorrelation $\mathbb{E}[s(t)s(t+\tau)] = R_s(t,\tau)$ are both periodic with period T_0 [24]. The autocorrelation $R_s(t,\tau)$ can then be expanded in a Fourier series whose coefficients, referred to as cyclic autocorrelations, are given by

$$R_s^\alpha(\tau) = \frac{1}{T_0}\int_{-T_0/2}^{T_0/2} R_s(t,\tau)e^{-j2\pi\alpha t}\mathrm{d}t, \tag{2}$$

where $\alpha = m/T_0, m \in \mathbb{Z}$. The cyclic spectrum is obtained by taking the Fourier transform of (2) with respect to τ, namely

$$S_s^\alpha(f) = \int_{-\infty}^{\infty} R_s^\alpha(\tau)e^{-j2\pi f\tau}\mathrm{d}\tau, \tag{3}$$

where α is the cyclic frequency and f is the angular frequency [24]. If there is more than one fundamental frequency T_0, then the cyclic spectrum contains harmonics (integer multiples) of each one [14]. These cyclic frequencies are related to the transmissions carrier frequencies and symbol rates as well as modulation types.

An alternative interpretation of the cyclic spectrum expresses it as the cross-spectral density $S_s^\alpha(f) = S_{uv}(f)$ of two frequency-shifted versions of $s(t)$, $u(t)$ and $v(t)$, such that

$$u(t) \triangleq s(t)e^{-j\pi\alpha t}, \quad v(t) \triangleq s(t)e^{+j\pi\alpha t}. \tag{4}$$

Then, from [25], it holds that

$$S_s^\alpha(f) = S_{uv}(f) = \mathbb{E}\left[S\left(f+\frac{\alpha}{2}\right)S^*\left(f-\frac{\alpha}{2}\right)\right]. \tag{5}$$

Stationary noise exhibits no cyclic correlation [14], [25], that is $S_n^\alpha(f) = 0$ for $\alpha \neq 0$. This property is the motivation for cyclostationary detection, in low SNR regimes in particular.

Since $s_i(t)$ are assumed to be zero-mean and uncorrelated, the cyclic spectrum of $x(t)$ is given by

$$S_x^\alpha(f) = \begin{cases} \sum_{i=1}^{N_{\text{sig}}} S_{s_i}^\alpha(f) & \alpha \neq 0 \\ \sum_{i=1}^{N_{\text{sig}}} S_{s_i}^0(f) + S_n^0(f) & \alpha = 0. \end{cases} \tag{6}$$

Denote by $[f_i^{(1)}, f_i^{(2)}]$ the right-side support of the ith transmission $s_i(t)$. Then, $B_i = f_i^{(2)} - f_i^{(1)}$ and $f_i = (f_i^{(1)} + f_i^{(2)})/2$. The support region in the (f,α) plane of the cyclic spectrum $S_{s_i}^\alpha(f)$ of such a bandpass cyclostationary signal is composed of four diamonds. More precisely, it holds that [14]

$$S_{s_i}^\alpha(f) = 0, \quad \text{for } \left||f| - \frac{|\alpha|}{2}\right| \leq f_i^{(1)} \text{ or } |f| + \frac{|\alpha|}{2} \geq f_i^{(2)}. \tag{7}$$

It follows from (6) that, besides the noise contribution at the cyclic frequency $\alpha = 0$, the support of $S_x^\alpha(f)$ is composed of $4N_{\text{sig}}$ diamonds, that is four diamonds for each transmission.

Our objective is to reconstruct $S_x^\alpha(f)$ from sub-Nyquist samples without any *a priori* knowledge on the support and modulations of $s_i(t), 1 \leq i \leq N_{\text{sig}}$. We show that the cyclic spectrum of non sparse signals can be recovered from samples obtained at $4/5$ of the Nyquist rate and for sparse signals, the sampling rate can be as low as $8/5$ of the Landau rate. We then estimate the number of transmissions N_{sig} present in $x(t)$, their carrier frequencies f_i and bandwidths B_i from these low rate samples.

III. SUB-NYQUIST SAMPLING

We adopt the MWC, a sub-Nyquist sampling scheme previously proposed in [7] for sparse multiband signals in conjunction with energy detection. The MWC is composed of M parallel channels. In each channel, an analog mixing front-end, where $x(t)$ is multiplied by a mixing function $p_i(t)$, aliases the spectrum, such that each band appears in baseband. The mixing functions $p_i(t)$ are required to be periodic with period T_p such that $f_p = 1/T_p \geq B$. The function $p_i(t)$ has a Fourier expansion

$$p_i(t) = \sum_{l=-\infty}^{\infty} c_{il}e^{j\frac{2\pi}{T_p}lt}. \tag{8}$$

In each channel, the signal goes through a lowpass filter with cut-off frequency $f_s/2$ and is sampled at the rate $f_s \geq f_p$, resulting in the samples $z_i[n]$. For the sake of simplicity, we choose $f_s = f_p$.

Repeating the calculations in [7], we derive the relation between the known discrete time Fourier transform (DTFT) of the samples $z_i[n]$ and the unknown $X(f)$

$$\mathbf{z}(\tilde{f}) = \mathbf{A}\mathbf{x}(\tilde{f}), \qquad \tilde{f} \in [0, f_s], \tag{9}$$

where $\mathbf{z}(\tilde{f})$ is a vector of length M with ith element $z_i(\tilde{f}) = Z_i(e^{j2\pi\tilde{f}T_s})$. The unknown vector $\mathbf{x}(\tilde{f})$ is given by

$$\mathbf{x}_i(\tilde{f}) = X(\tilde{f} + (i - \lceil N/2\rceil)f_p), \quad \tilde{f} \in [0, f_s], \tag{10}$$

for $1 \leq i \leq N$ with $N = \lceil f_{\text{Nyq}}/f_s\rceil$. The $M \times N$ matrix $\mathbf{A}$ contains the known coefficients c_{il} such that $\mathbf{A}_{il} = c_{i,-l} = c_{il}^*$. The resulting sampling rate is then

$$f_{tot} = Mf_s = \frac{M}{N}f_{\text{Nyq}}. \tag{11}$$

IV. CYCLIC SPECTRUM RECONSTRUCTION

We now provide a method to reconstruct the cyclic spectrum $S_x^\alpha(f)$ of $x(t)$ from correlations between shifted versions of $\mathbf{z}(\tilde{f})$, defined in (9). We also investigate recovery conditions.

IV-A. Relation Between Samples and the Cyclic Spectrum

From (9), we have

$$\mathbf{R}_{\mathbf{z}}^a(\tilde{f}) = \mathbf{A}\mathbf{R}_{\mathbf{x}}^a(\tilde{f})\mathbf{A}^H, \quad \tilde{f} \in [0, f_s - a], \tag{12}$$

for all $a \in [0, f_s]$, where $(.)^H$ is the Hermitian operation. Here,

$$\mathbf{R}_{\mathbf{x}}^a(\tilde{f}) = \mathbb{E}\left[\mathbf{x}(\tilde{f})\mathbf{x}^H(\tilde{f}+a)\right], \quad \mathbf{R}_{\mathbf{z}}^a(\tilde{f}) = \mathbb{E}\left[\mathbf{z}(\tilde{f})\mathbf{z}^H(\tilde{f}+a)\right]. \tag{13}$$

The entries in the matrix $\mathbf{R}_{\mathbf{x}}^{a}(\tilde{f})$ are correlations between shifted versions of the slices $\mathbf{x}(\tilde{f})$, namely correlations between frequency-shifted versions of $x(t)$. The variable a controls the shift between the slices, while $\tilde{f}$, running in the interval $[0, f_s - a]$, determines the specific frequency location within the slice.

We begin by investigating the link between the cyclic spectrum $S_x^{\alpha}(f)$ and the shifted correlations between the slices $\mathbf{x}(\tilde{f})$, namely the entries of $\mathbf{R}_{\mathbf{x}}^{a}(\tilde{f})$. We then show how the latter can be recovered from $\mathbf{R}_{\mathbf{z}}^{a}(\tilde{f})$ using (12). The alternative definition of the cyclic spectrum (5) implies that the elements in $\mathbf{R}_{\mathbf{x}}^{a}(\tilde{f})$ are equal to $S_x^{\alpha}(f)$ at the corresponding α and f. Indeed, it can easily be shown that

$$\mathbf{R}_{\mathbf{x}}^{a}(\tilde{f})_{(i,j)} = S_x^{\alpha}(f), \tag{14}$$

for

$$\begin{aligned} \alpha &= (j-i)f_s + a \\ f &= -\frac{f_{\text{Nyq}}}{2} + \tilde{f} - \frac{f_s}{2} + \frac{(j+i)f_s}{2} + \frac{a}{2}. \end{aligned} \tag{15}$$

Here, $\mathbf{R}_{\mathbf{x}}^{a}(\tilde{f})_{(i,j)}$ denotes the (i,j)th element of $\mathbf{R}_{\mathbf{x}}^{a}(\tilde{f})$. Our goal is then to recover $\mathbf{R}_{\mathbf{x}}^{a}(\tilde{f})$, for $a \in [0, f_s]$ and $\tilde{f} \in [0, f_s - a]$, since once $\mathbf{R}_{\mathbf{x}}^{a}(\tilde{f})$ is known, $S_x^{\alpha}(f)$ follows for all (α, f), using (14).

The structure of $\mathbf{R}_{\mathbf{x}}^{a}(\tilde{f})$, for a given $a \in]0, f_s]$ and $\tilde{f} \in [0, f_s - a]$ was analyzed in [26]. It was found that the non zero entries of $\mathbf{R}_{\mathbf{x}}^{a}(\tilde{f})$ are contained in its -1, 0 and 1-diagonals and -1, 0 and 1-anti diagonals. Besides, $\mathbf{R}_{\mathbf{x}}^{a}(\tilde{f})$ exhibits additional structure concerning the locations of these elements. Finally, $\mathbf{R}_{\mathbf{x}}^{a}(\tilde{f})$ contains at most $K = 2N_{\text{sig}}$ rows/columns that have non zero elements. Without any sparsity assumption, $K = N$. It follows that $\mathbf{R}_{\mathbf{x}}^{a}(\tilde{f})$ is $2K$-sparse with additional structure. A detailed analysis can be found in [26].

Since the non zero elements of $\mathbf{R}_{\mathbf{x}}^{a}(\tilde{f})$ only lie on the 3 main and anti-diagonals, (12) can be further reduced to

$$\mathbf{r}_{\mathbf{z}}^{a}(\tilde{f}) = (\bar{\mathbf{A}} \otimes \mathbf{A})\text{vec}(\mathbf{R}_{\mathbf{x}}^{a}(\tilde{f})) = (\bar{\mathbf{A}} \otimes \mathbf{A})\mathbf{B}\mathbf{r}_{\mathbf{x}}^{a}(\tilde{f}) \triangleq \mathbf{\Phi}\mathbf{r}_{\mathbf{x}}^{a}(\tilde{f}), \tag{16}$$

where $\bar{\mathbf{A}}$ denotes the conjugate matrix of $\mathbf{A}$ and

$$\mathbf{\Phi} = (\bar{\mathbf{A}} \otimes \mathbf{A})\mathbf{B}. \tag{17}$$

Here $\otimes$ is the Kronecker product, $\mathbf{r}_{\mathbf{z}}^{a}(\tilde{f}) = \text{vec}(\mathbf{R}_{\mathbf{z}}^{a}(\tilde{f}))$, where $\text{vec}(\cdot)$ denotes the column concatenation operation, and $\mathbf{B}$ is a selection matrix that selects the elements of the -1, 0 and 1-diagonals and anti-diagonals of $\mathbf{R}_{\mathbf{x}}^{a}(\tilde{f})$ from the vector $\text{vec}(\mathbf{R}_{\mathbf{x}}^{a}(\tilde{f}))$. The resulting $(6N-4) \times 1$ vector composed of these selected elements, denoted by $\mathbf{r}_{\mathbf{x}}^{a}(\tilde{f})$, is $2K$-sparse and its support presents additional structure. The case $a = 0$ corresponds to noisy recovery and a noise component needs to be added to (16); see [26].

IV-B. Cyclic Spectrum Recovery Conditions

Theorem 1 below derives sufficient conditions on the minimal number of channels M for perfect recovery of $\mathbf{R}_{\mathbf{x}}^{a}(\tilde{f})$, for any $a \in]0, f_s]$ and $\tilde{f} \in [0, f_s - a]$ in the presence of additive stationary noise. As stated above, for $a = 0$, the recovery is noisy.

Theorem 1. *If $\mathbf{A}$ is full spark and $M > \frac{8}{5}K$, then the system (16) has a unique solution for $a \in]0, f_s]$.*

Without any sparsity assumption, if $M > \frac{4}{5}N$, then we can perfectly recover the cyclic spectrum of $x(t)$. The minimal sampling rate is then

$$f_{\text{min}_0} = Mf_s = \frac{4}{5}Nf_s = \frac{4}{5}f_{\text{Nyq}}. \tag{18}$$

This means that even without any sparsity constraints on the signal, we can retrieve its cyclic spectrum from samples below the Nyquist rate, by exploiting its cyclostationary properties. A similar result was observed in [12] in the context of power spectrum reconstruction of wide-sense stationary signals in noiseless settings. There, it was shown that the power spectrum can be retrieved at half the Nyquist rate without any sparsity constraints. Here, we extend this result to cyclic spectrum reconstruction, which requires a higher rate.

If $x(t)$ is assumed to be sparse in the frequency domain, with $K = 2N_{\text{sig}} \ll N$, then the minimal sampling rate for perfect reconstruction of its cyclic spectrum is

$$f_{\text{min}} = Mf_s = \frac{16}{5}N_{\text{sig}}B = \frac{8}{5}f_{\text{Landau}}. \tag{19}$$

It was shown in [12], that the power spectrum of a stationary sparse signal can be perfectly recovered at its Landau rate. Again, the minimal sampling rate for cyclic spectrum recovery is slightly higher than the rate required for power spectrum reconstruction.

For $a \in]0, f_s]$, there is no noise component in (16), even if $x(t)$ is corrupted by additional stationary noise. For the corresponding cyclic frequencies, we can therefore achieve perfect recovery. In contrast, for $a = 0$, which corresponds to cyclic frequencies which are multiple of f_s, the recovery of the sparse vector is not perfect and is performed in the presence of bounded noise. In the simulations, we observe that, for detection purposes, this noisy recovery is satisfactory. Perfect recovery can be achieved by using a different sampling frequency at the expense of increased overall sampling rate by a factor of 2.

IV-C. Cyclic Spectrum Recovery

So far, we only discussed the conditions for perfect recovery of the cyclic spectrum, namely for (16) to have a unique solution. We now briefly present a cyclic spectrum's recovery method from low rate samples. For both sparse and non sparse signals, we use the support recovery paradigm from [6] that produces a finite system of equations, called multiple measurement vectors (MMV) from an infinite number of linear systems. This reduction is performed by the continuous to finite (CTF) block. From (16), for $a \in]0, f_s]$, we have

$$\mathbf{Q}^a = \mathbf{\Phi}\mathbf{Z}^a\mathbf{\Phi}^H \tag{20}$$

where

$$\mathbf{Q}^a = \int_{\tilde{f} \in \mathcal{F}_s} \mathbf{r}_{\mathbf{z}}^{a}(\tilde{f})\mathbf{r}_{\mathbf{z}}^{a\,H}(\tilde{f})\mathrm{d}\tilde{f}, \quad \mathbf{Z}^a = \int_{\tilde{f} \in \mathcal{F}_s} \mathbf{r}_{\mathbf{x}}^{a}(\tilde{f})\mathbf{r}_{\mathbf{x}}^{a\,H}(\tilde{f})\mathrm{d}\tilde{f}. \tag{21}$$

We then construct a frame $\mathbf{V}^a$ such that $\mathbf{Q}^a = \mathbf{V}^a(\mathbf{V}^a)^H$ by performing an eigendecomposition of $\mathbf{Q}^a$ and choosing $\mathbf{V}^a$ as the matrix of eigenvectors corresponding to the non zero eigenvalues. We can then define the following linear system

$$\mathbf{V}^a = \mathbf{\Phi}\mathbf{U}^a. \tag{22}$$

From [6] (Propositions 2-3), the support of the unique sparsest solution of (22) is the same as the support of $\mathbf{r}_{\mathbf{x}}^{a}(\tilde{f})$ in our original set of equations (16).

For the CTF stage, we extend the orthogonal matching pursuit (OMP) [9], [27] to account for the structure of $\mathbf{r}_{\mathbf{x}}^{a}(\tilde{f})$ for $a \neq 0$. In each iteration, we add an internal loop that, for a selected element originally from the diagonals of $\mathbf{R}_{\mathbf{x}}^{a}(\tilde{f})$, checks for a corresponding non-zero element from the anti-diagonals, and vice versa. The structured OMP method is formally presented in [26].

Once the support S is known, perfect reconstruction of the cyclic spectrum can be obtained as follows

$$\begin{aligned} (\hat{\mathbf{r}}_{\mathbf{x}}^{a})^S(\tilde{f}) &= \mathbf{\Phi}_S^{\dagger}\mathbf{r}_{\mathbf{z}}^{a}(\tilde{f}) \\ \hat{\mathbf{r}}_{\mathbf{x}_i}^{a}(\tilde{f}) &= 0 \quad \forall i \notin S, \end{aligned} \tag{23}$$

for all $a \in]0, f_s]$. Then, the cyclic spectrum $S_x^{\alpha}(f)$ is assembled using (14) for (f, α) defined in (15).

The carrier frequency and bandwidth estimation algorithm from [28] is then applied to the reconstructed cyclic spectrum. This approach is a simple parameter extraction method from the cyclic spectrum of

multiband signals that allows the estimation of several carriers and bandwidths simultaneously, as well as the number of transmissions N_{sig}. The proposed parameter estimation algorithm performs thresholding and clustering on the cyclic spectrum to estimate the location and width of the cyclic peaks, corresponds to the carrier f_i and bandwidth B_i, respectively. Details can be found in [28].

V. SIMULATION RESULTS

We now illustrate our sub-Nyquist cyclic spectrum reconstruction from sub-Nyquist samples. For comparison, we use the energy detection method based on power spectrum recovery from [12].

We consider $x(t)$ composed of $N_{\text{sig}} = 3$ BPSK transmissions, which have cyclic features at the locations $(f, \alpha) = (0, \pm f_c), (\pm f_c, \pm \frac{1}{T})$, where f_c is the carrier frequency and T is the symbol period [14]. Each transmission has bandwidth $B = 18$MHz and the carrier frequencies are drawn uniformly at random in $[0, \frac{f_{\text{Nyq}}}{2}]$, with $f_{\text{Nyq}} = 1$GHz. In this experiment, the selected carriers are $f_1 = 163.18$MHz, $f_2 = 209.69$MHz and $f_3 = 396.12$MHz. The SNR is set to -5dB. In the sampling stage, we use the MWC with $M = 9$ channels, each sampling at $f_s = 23.26$MHz. The overall sampling rate is therefore 210MHz, that is a little below twice the Landau rate and 21% of the Nyquist rate. Here, the theoretical minimal sampling rate is $f_{\text{min}} = 172.8$MHz.

Figure 1 presents the original and reconstructed power spectrum using $P = 100$ frames. We observe that the signal's spectrum was not perfectly recovered due to the noise. The reconstructed cyclic spectrum, including the power spectrum, estimated over $P = 100$ frames as well, is shown in Fig. 2 and the section corresponding to $f = 0$, before and after clustering, can be seen in Fig. 3. The cyclic peaks at the locations $(f, \alpha) = (0, \pm f_i)$, for $i = 1, 2, 3$ can be observed in both figures. The estimated carriers and bandwidths are reported in the figures' legend. Clearly, cyclostationary detection succeeded where energy detection failed.

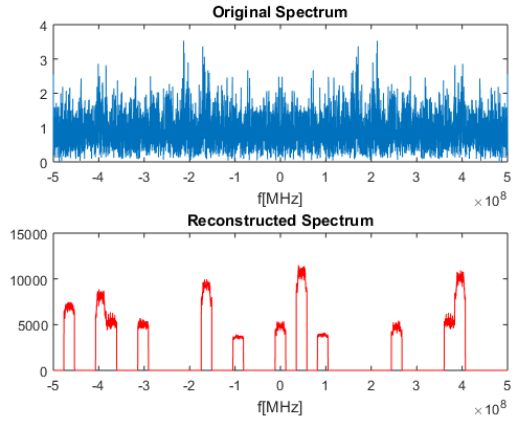

Fig. 1. Original and reconstructed power spectrum. Using energy detection, we obtain $\hat{N}_{\text{sig}} = 5$ signals, with estimated carriers (in MHz) $\hat{f}_1 = 93.04$, $\hat{f}_2 = 162.82$, $\hat{f}_3 = 255.86$, $\hat{f}_4 = 383.89$MHz, $\hat{f}_5 = 465.21$ and estimated bandwidths (in MHz) $\hat{B}_1 = \hat{B}_2 = \hat{B}_3 = \hat{B}_5 = 23.1$, $\hat{B}_4 = 46.3$.

Next, we investigate the performance of our carrier frequency and bandwidth estimation algorithm from sub-Nyquist samples with respect to SNR and compare it to energy detection. We consider $x(t)$ composed of $N_{\text{sig}} = 3$ BPSK transmissions with identical parameters as in the previous section. The sampling parameters remain the same as well. In each experiment, we draw the carrier frequencies uniformly at random and generate the transmissions. Fig. 4 shows the probability

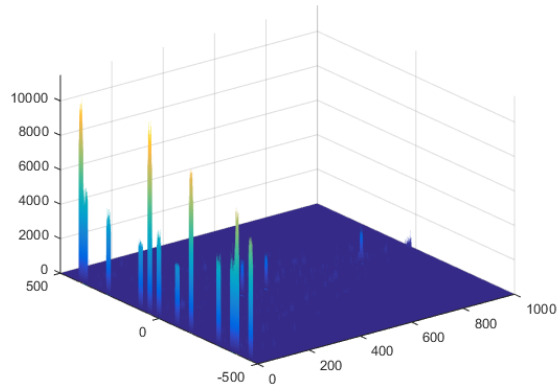

Fig. 2. Reconstructed cyclic spectrum.

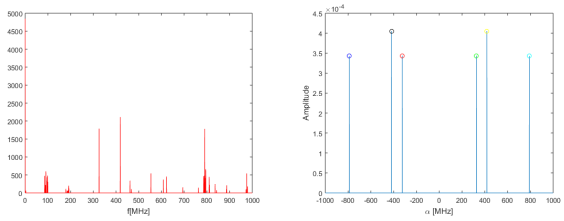

Fig. 3. Reconstructed cyclic spectrum for $f = 0$, $S_x^{\alpha}(0)$, as a function of α (left), clustering (right). The estimated number of clusters is 6, yielding $\hat{N}_{\text{sig}} = 3$. The estimated carriers (in MHz) using cyclostationary detection are $\hat{f}_1 = 162.66$, $\hat{f}_2 = 209.19$, $\hat{f}_3 = 395.11$, and corresponding bandwidths (in MHz) $\hat{B}_1 = 17.4$, $\hat{B}_2 = 17.4$, $\hat{B}_3 = 17.0$.

of detection of both cyclostationary (blue) and energy (red) detection. A detection is reported if the distance between the true and recovered carrier frequencies is below 10 times the frequency resolution. Clearly, cyclostationarity outperforms the energy approach in terms of probability of detection.

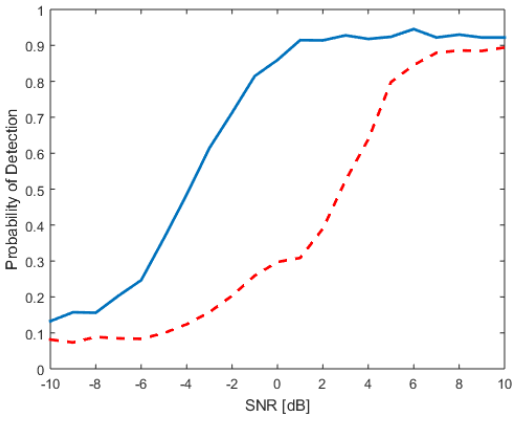

Fig. 4. Probability of detection - cyclostationary vs. energy detection.

VI. REFERENCES

[1] J. Mitola, "Software radios: Survey, critical evaluation and future directions," *IEEE Aerosp. Electron. Syst. Mag*, vol. 8, pp. 25–36, Apr. 1993.

[2] E. Axell, G. Leus, E. Larsson, and H. Poor, "Spectrum sensing for cognitive radios: State-of-the-art and recent advances," *IEEE Signal Process. Magazine*, vol. 29, pp. 101–116, May 2012.

[3] FCC, "Spectrum policy task force report: Federal communications commission, tech. rep. 02-135. [online]," *http://www.gov/edocs_public/attachmatch/DOC228542A1.pdf*, Nov. 2002.

[4] M. McHenry, "NSF spectrum occupancy measurements project summary. shared spectrum co., tech. rep. [online]," *http://www.sharedspectrum.com*, Aug. 2005.

[5] R. I. C. Chiang, G. B. Rowe, and K. W. Sowerby, "A quantitative analysis of spectral occupancy measurements for cognitive radio," *IEEE Vehicular Technology Conf.*, pp. 3016–3020, Apr. 2007.

[6] M. Mishali and Y. C. Eldar, "Blind multi-band signal reconstruction: Compressed sensing for analog signals," *IEEE Trans. on Signal Process.*, vol. 57, no. 3, pp. 993–1009, Mar. 2009.

[7] ——, "From theory to practice: Sub-Nyquist sampling of sparse wideband analog signals," vol. 4, no. 2, pp. 375–391, Apr. 2010.

[8] ——, "Sub-Nyquist sampling: Bridging theory and practice," *IEEE Signal Proc. Magazine*, vol. 28, no. 6, pp. 98–124, Nov. 2011.

[9] Y. C. Eldar, *Sampling Theory: Beyond Bandlimited Systems*. Cambridge University Press, 2015.

[10] M. A. Lexa, M. E. Davies, J. S. Thompson, and J. Nikolic, "Compressive power spectral density estimation," *IEEE ICASSP*, vol. 57, pp. 22–27, May 2011.

[11] D. D. Ariananda and G. Leus, "Compressive wideband power spectrum estimation," *IEEE Trans. on Signal Process.*, vol. 60, pp. 4775–4789, Sept. 2012.

[12] D. Cohen and Y. C. Eldar, "Sub-Nyquist sampling for power spectrum sensing in cognitive radios: A unified approach," *IEEE Trans. on Signal Process.*, vol. 62, pp. 3897–3910, Aug. 2014.

[13] E. Arias-Castro and Y. C. Eldar, "Noise folding in compressed sensing," *IEEE Signal Process. Letters*, vol. 18, no. 8, pp. 478–481, Aug. 2011.

[14] W. Gardner, *Statistical spectral analysis: a non probabilistic theory*. Prentice Hall, 1988.

[15] C. M. Spooner and R. B. Nicholls, *Spectrum sensing based on spectral correlation, in: B. Fette (Ed.), Cognitive Radio Technology, 2nd ed. (Chapter 18)*. Elsevier, 1909.

[16] S. Haykin, D. J. Thomson, and J. H. Reed, "Spectrum sensing for cognitive radio," *Proceedings of the IEEE*, vol. 97, pp. 849–877, 2009.

[17] A. Napolitano, "Cyclostationary: New trends and applications," *Signal Process.*, vol. 120, pp. 385–408, Jan. 2016.

[18] Z. Tian, "Cyclic feature based wideband spectrum sensing using compressive sampling," *IEEE ICC*, pp. 1–5, Jun. 2011.

[19] Z. Tian, Y. Tafesse, and B. M. Sadler, "Cyclic feature detection with sub-nyquist sampling for wideband spectrum sensing," *IEEE Journal on Sel. Topics Signal Process.*, vol. 6, no. 1, pp. 58–69, Feb. 2012.

[20] S. A. Razavi, M. Valkama, and D. Cabric, "High-resolution cyclic spectrum reconstruction from sub-Nyquist samples," *IEEE SPAWC*, pp. 250–254, Jun. 2013.

[21] G. Leus and Z. Tian, "Recovering second-order statistics from compressive measurements," *IEEE CAMSAP*, pp. 337–340, Dec. 2011.

[22] D. D. Ariananda and G. Leus, "Non-uniform sampling for compressive cyclic spectrum reconstruction," *IEEE ICASSP*, pp. 41–45, 2014.

[23] M. Mishali, Y. C. Eldar, O. Dounaevsky, and E. Shoshan, "Xampling: Analog to digital at sub-nyquist rates," *IET Circuits, Devices & Systems*, vol. 5, no. 1, pp. 8–20, Jan. 2011.

[24] W. A. Gardner, A. Napolitano, and L. Paura, "Cyclostationarity: Half a century of research," pp. 639–697, 2006.

[25] A. Papoulis, *Probability, Random Variables, and Stochastic Processes*. McGraw Hill, 1991.

[26] D. Cohen and Y. C. Eldar, "Sub-Nyquist cyclostationary detection for cognitive radio," *CoRR*, vol. abs/1604.02659, 2016. [Online]. Available: http://arxiv.org/abs/1604.02659

[27] Y. C. Eldar and G. Kutyniok, *Compressed Sensing: Theory and Applications*. Cambridge University Press, 2012.

[28] D. Cohen, L. Pollak, and Y. C. Eldar, "Carrier frequency and bandwidth estimation of cyclostationary multiband signals," *IEEE ICASSP*, Mar. 2016.